Cancer cell–derived microparticles bearing P-selectin glycoprotein ligand 1 accelerate thrombus formation in vivo

Grace M. Thomas,[1,2] Laurence Panicot-Dubois,[1,2] Romaric Lacroix,[3] Françoise Dignat-George,[3] Dominique Lombardo,[1,2] and Christophe Dubois[1,2]

[1]Institut National de la Santé et de la Recherche Médicale (INSERM) UMR911, Centre de Recherche en Oncologie Biologique et Oncopharmacologie, 13385 Marseille, France
[2]Aix-Marseille Université, Faculté de Médecine La Timone, 13385 Marseille, France
[3]INSERM UMR608, Laboratoire d'Hématologie et d'Immunologie, 13385 Marseille, France

Recent publications have demonstrated the presence of tissue factor (TF)–bearing microparticles (MPs) in the blood of patients suffering from cancer. However, whether these MPs are involved in thrombosis remains unknown. We show that pancreatic and lung cancer cells produce MPs that express active TF and P-selectin glycoprotein ligand 1 (PSGL-1). Cancer cell–derived MPs aggregate platelets via a TF-dependent pathway. In vivo, cancer cell–derived MPs, but not their parent cells, infused into a living mouse accumulate at the site of injury and reduce tail bleeding time and the time to occlusion of venules and arterioles. This thrombotic state is also observed in mice developing tumors. In such mice, the amount of circulating platelet-, endothelial cell–, and cancer cell–derived MPs is increased. Endogenous cancer cell–derived MPs shed from the growing tumor are able to accumulate at the site of injury. Infusion of a blocking P-selectin antibody abolishes the thrombotic state observed after injection of MPs or in mice developing a tumor. Collectively, our results indicate that cancer cell–derived MPs bearing PSGL-1 and TF play a key role in thrombus formation in vivo. Targeting these MPs could be of clinical interest in the prevention of thrombosis and to limit formation of metastasis in cancer patients.

CORRESPONDENCE
Christophe Dubois:
christophe.dubois@univmed.fr

Abbreviations used: MP, microparticle; PPP, platelet-poor plasma; PSGL-1, P-selectin glycoprotein ligand 1; Qdot, quantum dot ; TF, tissue factor.

The association between the development of metastasis and the risk of thrombotic complications has been documented since 1865. Armand Trousseau was the first to establish a direct correlation between thrombophlebitis and the development of cancer (Trousseau, 1865). A rather common complication and one of the leading causes of death in patients with cancer is the risk of developing thromboembolic diseases (Kakkar and Williamson, 1999; Stein et al., 2006; Schiavetti et al., 2008). The incidence of thrombosis is high in adenocarcinomas such as ovarian, prostate, lung, and gastrointestinal carcinomas (Blom et al., 2006b), and it is particularly high (up to 57%) in patients suffering from pancreatic cancer (Sack et al., 1977; Blom et al., 2006a). In the latter case, thromboembolic diseases are the second most common cause of mortality, accounting for 44% of total deaths after cancer progression (Neoptolemos et al., 2001). The recurrence of thrombotic complications may also be the first manifestation of underlying malignant disease (Prandoni et al., 1992).

The pathogenesis of the thrombotic state in cancer is associated with the generation of a local and systemic hypercoagulable/thrombotic state that confers a growth advantage to tumor cells. It is now known that activation of the coagulation cascade and aggregation of blood platelets around cancer cells protects the cells from the different degradative pathways present in the blood, and also facilitates dissemination of cancer cells to various sites of metastasis (Gasic et al., 1976; Sierko and Wojtukiewicz, 2007). This supports a model in which the presence of tissue factor (TF), generation of thrombin, and activation of platelets favor the aggressive

The Rockefeller University Press $30.00
J. Exp. Med. Vol. 206 No. 9 1913-1927
www.jem.org/cgi/doi/10.1084/jem.20082297

biology of cancer. Nevertheless, the cause of this association remains unclear.

Different reports suggest a potential role for circulating microparticles (MPs) in the establishment of a thrombotic state in cancer (Kim et al., 2003; Del Conde et al., 2007; Tilley et al., 2008). MPs are defined as cell-derived membrane fragments and range in size from 0.1 to 1 µm in diameter. They are characterized by their presence at the surface of negative phospholipid moieties that are essential for initiation of blood coagulation (Ghosh et al., 2008); they also bear at least one of the antigenic markers distinctive of the parent cell (Abid Hussein et al., 2003). Aggregated platelets, leukocytes, erythrocytes, and endothelial lineages constitute the most important sources of circulating MPs under many pathophysiological situations, including thrombosis, inflammation, and angiogenesis (Müller et al., 2003). Recent clinical studies have shown that the concentration of circulating TF-bearing MPs is significantly greater in patients with cancer (Tilley et al., 2008), including patients with pancreatic cancer (Del Conde et al., 2007; Hron et al., 2007; Tesselaar et al., 2007), suggesting that these MPs may be responsible for the thrombotic state associated with cancers. Meanwhile, the cellular origins of such MPs have not been determined (Hron et al., 2007; Zwicker et al., 2007; Langer et al., 2008) and may include platelets (Hron et al., 2007; Tesselaar et al., 2007), cancer cells (Dvorak et al., 1981), or monocytes (Falati et al., 2003; Myers et al., 2003; Vandendries et al., 2007). At their surface, platelet-derived MPs express activated integrins (e.g., $\alpha_{IIb}\beta_3$ or $\alpha_v\beta_3$) and receptors (i.e., GPVI and GPIb-IX-V) known to be involved in thrombus formation. Monocyte-derived MPs that have been isolated, labeled, and infused into a recipient mouse accumulate at the site of a laser-induced injury by binding to P-selectin expressed on activated platelets through P-selectin glycoprotein ligand 1 (PSGL-1; Falati et al., 2003; Vandendries et al., 2007). To date, no study has determined the role of cancer cell–derived MPs in thrombus formation in vivo.

In the present study, we hypothesize that cancer cell–derived MPs bearing PSGL-1 are involved in the development of a thrombotic state. We demonstrate that pancreatic cancer cells are able to produce MPs in vitro that express active TF and PSGL-1. We show that cancer cell–derived MPs circulate in the bloodstream and accumulate at the site of injury in a P-selectin–dependent manner in vivo. Finally, we observe that cancer cell–derived MPs, but not their parental cells, accelerate thrombus formation in a mouse model of cancer.

RESULTS

Human and mouse pancreatic and lung cancer cell lines are able to shed MPs that express TF and PSGL-1 in vitro

To determine whether pancreatic or lung cancer cells could shed MPs, ultracentrifuged supernatants of human (SOJ-6) and mouse (Panc02) adenocarcinoma pancreatic cell lines or mouse Lewis lung carcinoma cancer cell lines (LLC1) were evaluated by flow cytometry. All cancer cell lines produced vesicles ranging in size from 0.4 to 1 µm in diameter, and these particles were able to bind annexin V (Fig. 1 A). Previous

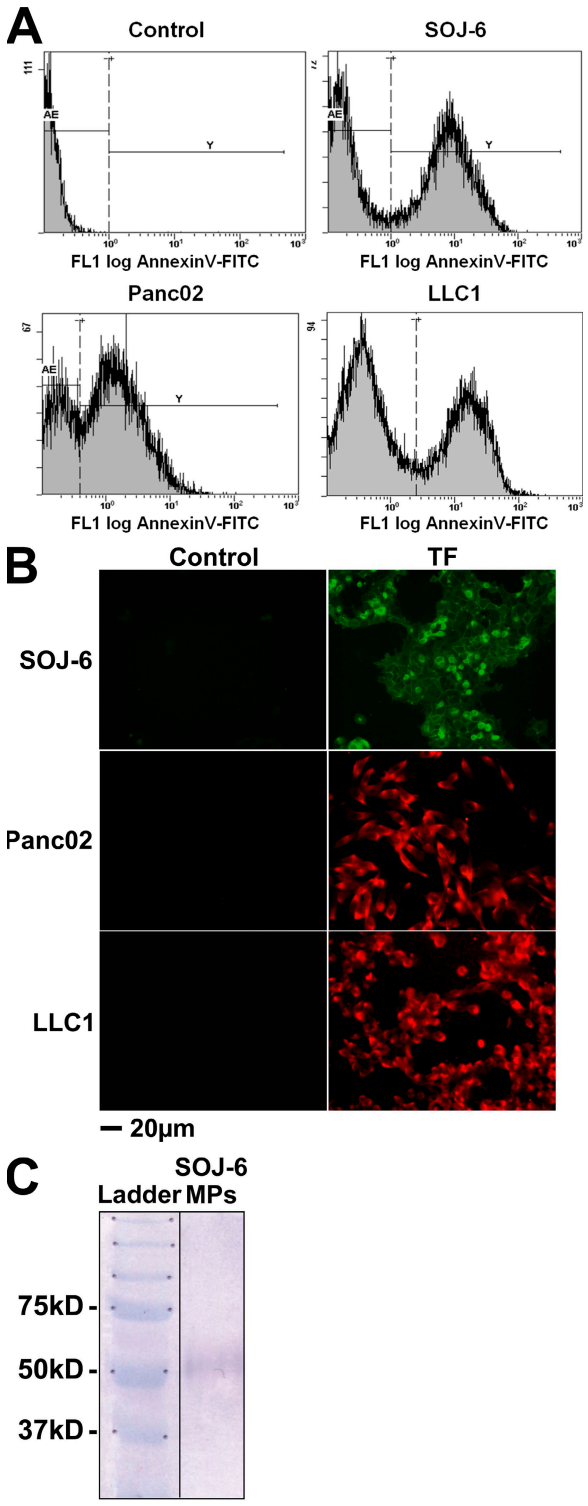

Figure 1. Pancreatic and lung cancer cell lines shed MPs that express TF in vitro. (A) Flow cytometry analysis showing annexin V–FITC labeling of SOJ-6, Panc02, and LLC1 cell–derived MPs. Negative controls were realized without addition of calcium. (B) Immunofluorescence microscopy of cancer cells using an anti-TF antibody. (C) Western blot analysis of protein extracts from SOJ-6–derived MPs with a specific anti-TF antibody. All of the experiments were independently performed three times.

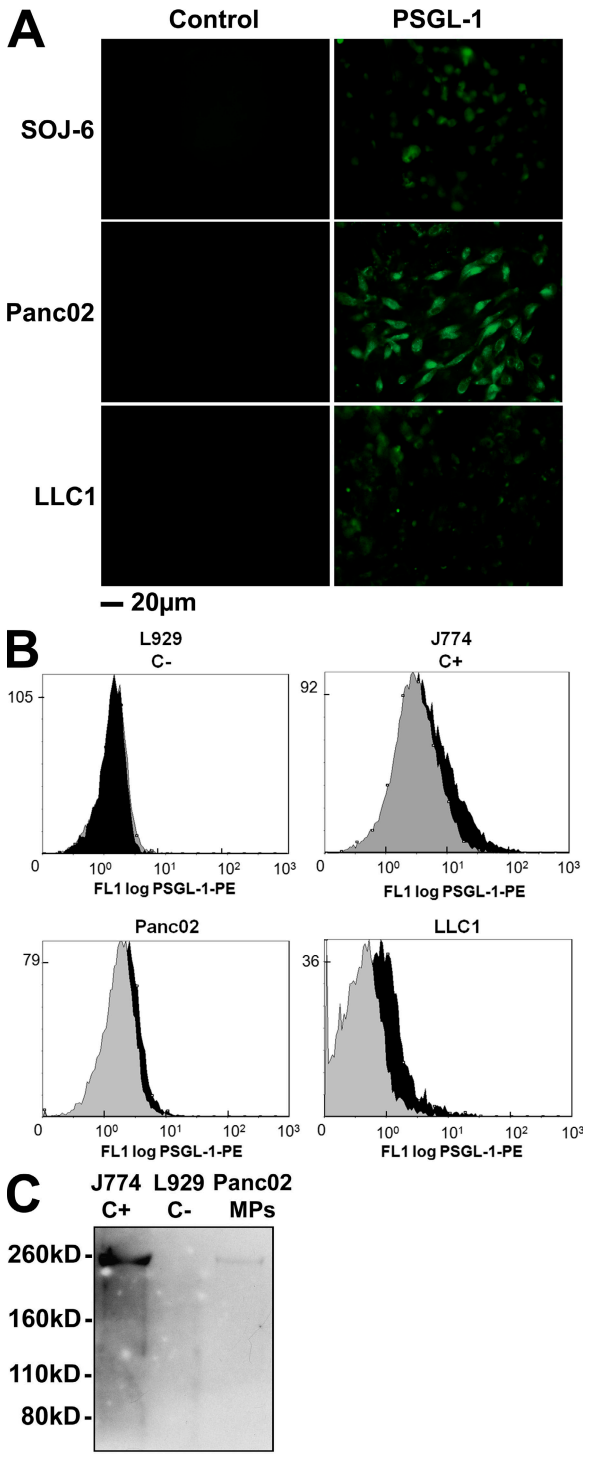

Figure 2. Pancreatic and lung cancer cell–derived MPs express PSGL-1. (A) Immunofluorescence microscopy of SOJ-6, Panc02, and LLC1 cells with an antibody directed against PSGL-1 and an Alexa Fluor 488–conjugated secondary antibody. Incubation with the secondary antibody alone served as a negative control. (B) Flow cytometric analysis of J774 (C+), L929 (C−), Panc02-, and LLC1-derived MPs labeled both with annexin V–FITC and with an anti–PSGL-1 PE-conjugated antibody. PSGL-1$^+$ MPs are represented by the black histogram. Negative controls were obtained by excluding calcium from the annexin V labeling and in the presence of an irrelevant PE-conjugated IgG (gray histogram). (C) Western blot analysis of Panc02-derived MPs (Panc02 MPs) and J774 (C+) and L929 (C−) cells with a specific anti–PSGL-1 antibody. All of the experiments were independently performed three times.

reports have shown that TF is present on the surface of cancer cell lines (Haas et al., 2006; Khorana et al., 2007). Accordingly, we observed that SOJ-6, Panc02, and LLC1 cancer cells express TF on their surface by immunofluorescence (Fig. 1 B). TF was also detected by Western blotting of lysates obtained from pancreatic cancer cell–derived MPs (Fig. 1 C). Identical results were obtained with all other pancreatic adenocarcinoma (BxPC-3) and carcinoma (MiaPaCa-2, PANC-1, and LLC1) cell lines studied. Monocyte-derived MPs have been shown to express PSGL-1 (Falati et al., 2003; Myers et al., 2003). Double labeling with annexin V as a positive control revealed that Panc02 and LLC1 cancer cells (Fig. 2 A), as well as Panc02- and LLC1-derived MPs (Fig. 2 B), express PSGL-1 but not P-selectin (not depicted) on their surface. PSGL-1 was also detected by Western blotting in lysates obtained from pancreatic cancer cell– and monocyte-derived MPs (Fig. 2 C). In contrast, no signal was detected by flow cytometry analysis or Western blotting when mouse fibroblast–derived MPs (L929 cell lines) were studied. We conclude that pancreatic and lung cancer cells can shed MPs that constitutively express active TF and PSGL-1.

Cancer cell–derived MPs, but not their parental cells, modulate thrombus formation in vivo

We have previously described the kinetics of thrombus formation in mice after an injury induced by topical application of an $FeCl_3$ solution (Dubois et al., 2006b). To determine the involvement of MPs in thrombus formation in vivo, experiments we performed using a fibered fluorescent microscope that allows for real-time in vivo imaging after excitation at 660 nm. We examined thrombus formation induced by exposure of the adventitial surface of the mouse mesenteric vessels to 10% $FeCl_3$ for 5 min. Under these conditions, platelets began to accumulate in injured vessels between 5 and 15 min after $FeCl_3$ exposure (Fig. 3 A). Only three out of the eight wild-type mice studied formed occlusive thrombi during the 35-min experiment (Fig. 3 B). When Panc02 cancer cell–derived MPs (0.2 μg/g/mouse corresponding to 18,000 MPs/g/mouse) were infused into the bloodstream 5 min before topical application of $FeCl_3$, platelets began to accumulate 1–5 min after induction of the injury, leading to occlusion of the arterioles between 3 and 10 min after injury (Fig. 3 A). The median time to occlusion of the arteriole in this condition was 6 min ($P < 0.01$; Fig. 3 B). Similar results were observed after infusion of LLC1-derived MPs (0.08 μg/g/mouse, corresponding to 18,000 MPs/g/mouse), with a median time to occlusion of the arteriole of 12 min ($P < 0.05$; Fig. 3 B). The median time to arteriole occlusion was significantly shorter than the median time to occlusion observed without infusion of MPs ($P < 0.05$). These results indicate that infusion of cancer

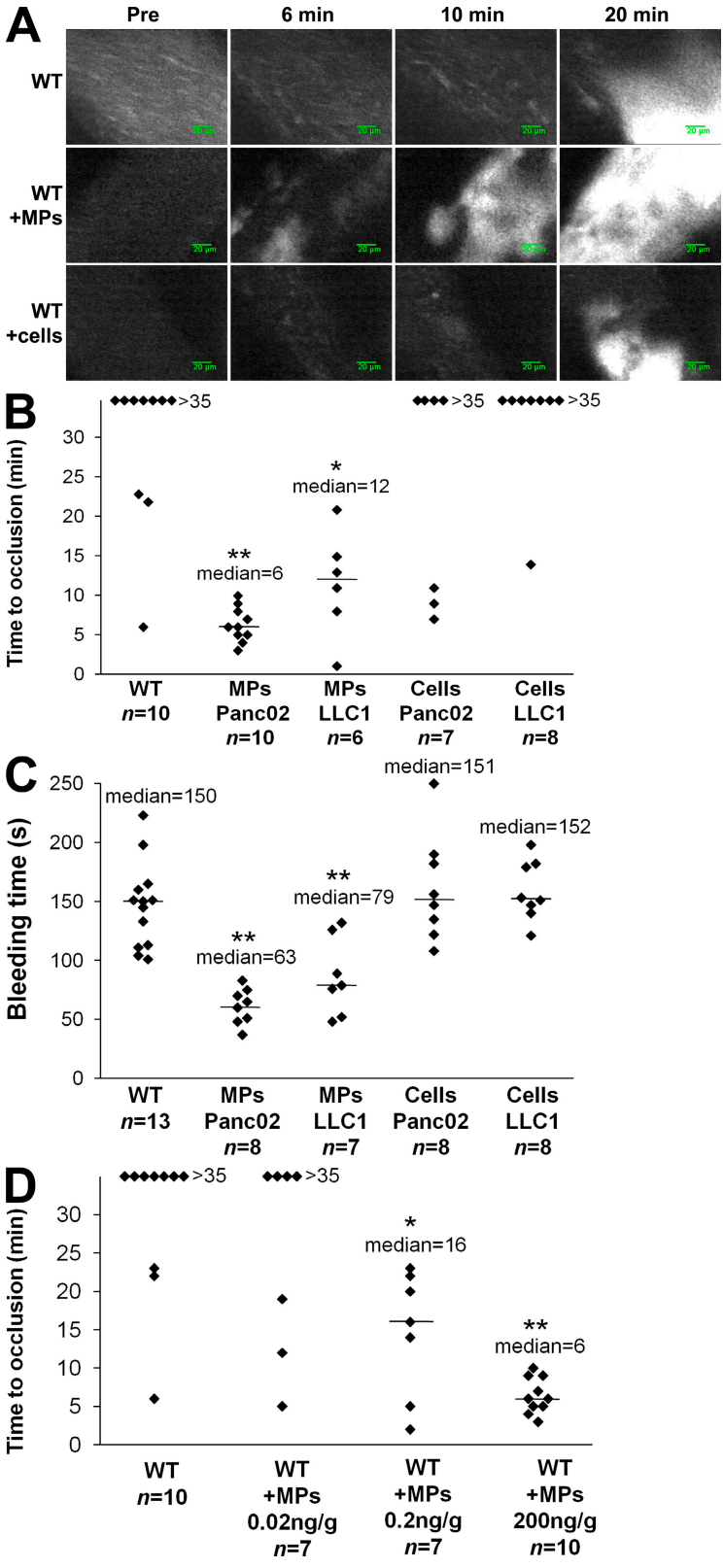

Figure 3. Cancer cell–derived MPs accelerate thrombus formation in vivo. Thrombus formation was assessed after infusion of Alexa Fluor 660–conjugated anti-CD41 antibody into wild-type mice in the presence of Panc02-derived MPs (MPs Panc02, 0.2 µg of MP-associated proteins/g/mouse), LLC1-derived MPs (MPs LLC1, 0.08 µg of MP-associated proteins/g/mouse), or Panc02 cells (Cells Panc02, 5,000 cells/g/mouse) or LLC1 cells (Cells LLC1, 5,000 cells/g/mouse). Injury of the mesenteric vessels was induced with 10% $FeCl_3$ for 5 min. (A) Representative composite images of fluorescence depicting

cell–derived MPs affected the kinetics of thrombus formation. To determine whether cancer cells may also be involved in thrombus formation, we determined the time to occlusion in arterioles after infusion of cancer cells (5,000 cells/g/mouse, equivalent to the maximum concentration of cells that may be infused without altering blood flow; not depicted; Fig. 3 A). In this condition, no statistical difference was found in comparison with the kinetics observed when wild-type mice were injured. Indeed, platelet accumulation was detected between 5 and 10 min after injury. Only three out of seven mice studied after infusion of Panc02 cells and only one out of eight mice studied after infusion of LLC1 cells formed occlusive thrombi (Fig. 3 B). To confirm the involvement of cancer cell–derived MPs in thrombus formation, tail bleeding time experiments were performed as previously described (Panicot-Dubois et al., 2007). After injection with Panc02- and LLC1-derived MPs, the median tail bleeding time observed in wild-type mice was 63 s ($n = 8$) and 79 s ($n = 7$), respectively. These values were significantly lower ($P < 0.01$) than the bleeding times (close to 150 s) obtained for wild-type mice that were not infused with cells or MPs ($n = 13$), wild-type mice infused with Panc02 cells ($n = 8$), or wild-type mice infused with LLC1 cells ($n = 8$; Fig. 3 C). We next determined the number of MPs sufficient enough to affect kinetics of thrombosis. We observed that an amount as low as 0.2 ng/g/mouse of cancer cell–derived MPs significantly accelerated kinetics of thrombosis in vivo in our model (Fig. 3 D). Collectively, these results indicate that infusion of cancer cell–derived MPs, but not infusion of their parental cells, accelerates thrombus growth in vivo, suggesting that cancer cell–derived MPs may participate in thrombus formation.

To determine whether cancer cell–derived MPs accumulate at the site of $FeCl_3$-induced injury in vivo, MPs were isolated, labeled with the DiD fluorochrome, and infused into a recipient mouse. First, we determined the half-life of exogenous MPs in the blood circulation of healthy mice (Fig. 4 A). The results show that 50% of exogenous MPs were eliminated from the blood circulation in <15 min, confirming the results previously described for erythrocyte-derived MPs infused into the rat (Willekens et al., 2005). After infusion of exogenous MPs and induction of a chemical injury to mesenteric arterioles, a fluorescent signal corresponding to DiD-labeled MPs was detected (Fig. 4 B). This accumulation of cancer cell–derived MPs at the site of injury was further confirmed by intravital microscopy (Dubois et al., 2007; Panicot-Dubois et al., 2007). Using such a system, we simultaneously imaged DiO-labeled cancer-derived MPs (0.2 μg/g/mouse, corresponding to 18,000 MPs/g/mouse) and DiD-labeled cancer cells (5,000 Panc02 cells/g/mouse) infused into the bloodstream of a recipient mouse. Both cancer cell–derived MPs and cancer cells were detected circulating in the blood (Fig. 4 C). However, only cancer cell–derived MPs were found to accumulate at the site of the $FeCl_3$-induced injury. 8 min after injury, the number of exogenous MPs accumulating at the site of injury increased, indicating that thrombus-associated MPs remained in the animal for a longer time period than did circulating MPs (Fig. 4 C). We conclude that cancer cell–derived MPs, but not their parental cells, accumulate at the site of injury in vivo and accelerate thrombus growth.

Characterization of a thrombotic state in mice developing ectopic tumors

Next, we created a mouse model of cancer induced by subcutaneous injection of pancreatic (Panc02) or lung cancer (LLC1) cells. 5 wk after induction of the ectopic tumor, the number of endogenous circulating MPs in both healthy mice and mice developing tumors were compared by flow cytometry analysis. To characterize the cellular origin of MPs, we first labeled MPs using antibodies specific for platelets ($CD41^+$), erythrocytes ($TER\ 119^+$), leukocytes ($CD45^+$), cells likely of endothelial origin ($CD31^+CD41^-$), and cancer cells ($MUC\text{-}1^+$). The data are presented in Table I (see also Fig. S1). As expected, the number of endogenous circulating annexin V^+ MPs was significantly increased in mice developing tumors in comparison with control mice (median = 9,383 MPs/μl and 10,018 MPs/μl of plasma for Panc02- and LLC1-induced-tumor mice, respectively, and 8,951 MPs/μl of plasma in control mice; $P < 0.05$). The amount of platelet- and endothelial cell–derived MPs was significantly increased in mice developing tumors in comparison with control mice. However, neither the number of leukocyte-derived circulating MPs nor the quantity of endogenous erythrocyte-derived MPs increased in comparison with the control. We also addressed the presence of endogenous circulating cancer cell–derived MPs using Muc-1, a protein that is highly expressed in various epithelial cancers. As expected, the amount of Muc-1–bearing MPs was significantly increased in tumor-induced mice in comparison with healthy mice. We also detected MPs bearing the carbohydrate CA19-9, which is highly expressed in lung and pancreatic cancers. Of note, this antigen was only present on MPs in blood obtained from Panc02- and LLC1-tumor-induced

thrombus formation of labeled platelet accumulation (white) on mesenteric vessels (Pre, before injury). (B) Time to vessel occlusion reported in minutes for mesenteric arterioles in wild-type mice ($n = 10$ thrombi in 10 mice), wild-type mice infused with Panc02-derived MPs ($n = 10$ thrombi in 7 mice), or with LLC1-derived MPs ($n = 6$ thrombi in 6 mice), Panc02 cells ($n = 7$ thrombi in 7 mice), or LLC1 cells ($n = 8$ thrombi in 8 mice). (C). Bleeding time in seconds determined in wild-type mice ($n = 13$ mice), wild-type mice infused with Panc02-derived MPs ($n = 8$ mice), or with LLC1-derived MPs ($n = 7$ mice), Panc02 cells ($n = 8$ mice), or LLC1 cells ($n = 8$ mice). (D) Times to arteriole occlusion were observed in wild-type mice ($n = 10$ thrombi in 10 mice) and in wild-type mice infused with different concentrations of Panc02-derived MPs (MPs 0.02 ng/g/mouse, $n = 7$ thrombi in 6 mice; MPs 0.2 ng/g mouse, $n = 7$ thrombi in 7 mice; and MPs 200 ng/g mouse, $n = 10$ thrombi in 9 mice). Horizontal bars indicate median values. Experiments were independently performed 10 times (A and B) and at least six times (C and D). **, $P < 0.01$; *, $P < 0.05$.

mice (Table I). Because we have previously observed that Panc02- and LLC1-derived MPs express PSGL-1 on their surface (Fig. 2) and because the quantity of leukocyte-derived MPs, which also bear PSGL-1, was not increased in tumor-induced mice in comparison with control mice, we determined the quantity of circulating PSGL-1–bearing MPs in the different populations of mice. The number of MPs bearing PSGL-1 was significantly increased in mice developing tumors in comparison with healthy mice. Collectively, our results indicate that the elevation of endogenous cell–derived MPs positive for annexin V results from a selective increase in MPs originating from platelets, endothelial cells, and tumor cells.

Tail bleeding times were significantly reduced in mice developing a tumor (median times for mice that received Panc02 or LLC1 cancer cells were 70 and 78 s, respectively) in comparison with mice that did not (median time = 150 s; $P < 0.01$; Fig. 5 A). We determined the kinetics of thrombus formation after $FeCl_3$ injury to both the mesenteric arterioles and venules of control and tumor-bearing mice (Fig. 5 B). A significant decrease in the time to occlusion of the arterioles ($P < 0.05$; Fig. 5 C) and venules ($P < 0.05$; Fig. 5 D) was observed in mice developing tumors (a median time to occlusion of 8 and 15 min in arterioles and 13 and 8 min in venules in mice developing Panc02- and LLC1-induced tumors, respectively) in comparison with control mice (median time > 35 and 18 min in arterioles and venules, respectively). Interestingly, the tail bleeding time and time to occlusion of arterioles and venules were similar in mice developing tumors (median volume = 239 mm^3) and mice for which Panc02-derived MPs were infused into the circulation (compare Fig. 3 B with 5 C and Fig. 3 C with 5 A). Furthermore, we did not observe any linear correlation between the volume of the tumor and the bleeding time (Fig. 5 E). Our results indicate that the presence of an ectopic tumor in mice increases the quantity of MPs present in the bloodstream and accelerates thrombus formation, as compared with healthy mice.

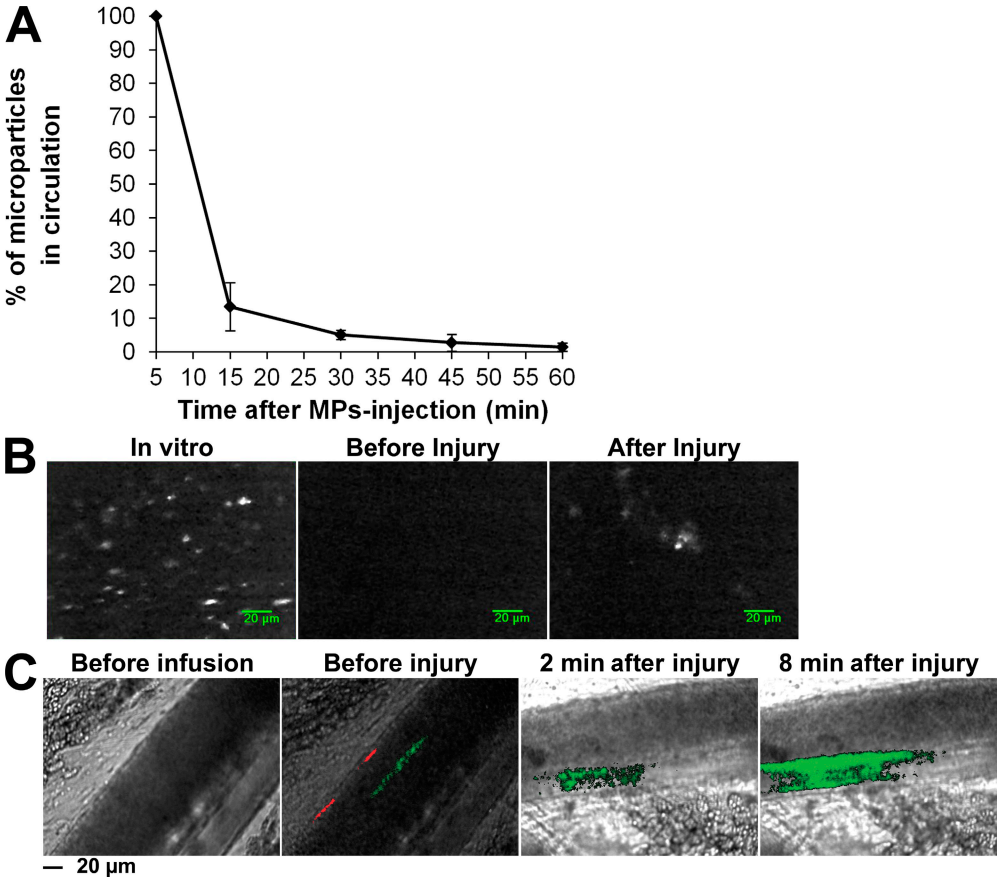

Figure 4. Cancer cell–derived MPs accumulate at the site of injury in mice. (A) Half-life of DiO-labeled Panc02-derived MPs in the blood circulation of a healthy mouse ($n = 4$ mice, performed independently) reported as the mean ± SD. (B) Imaging of DiD-labeled Panc02-derived MPs using fibered fluorescence microscopy. Panc02-derived MPs were labeled with DiD (left) before infusion into the blood circulation of a living mouse. Although no fluorescent signal was detected in the microcirculation before injury (middle), MPs were detected accumulating at the site of $FeCl_3$-induced injury (right). Images are representative of six injuries performed in three mice, independently. (C) Intravital videomicroscopy visualization of mesenteric vessels. DiO-labeled MPs (depicted in green; 0.2 µg of MP-associated proteins/g/mouse) and their DiD-labeled parental cells (depicted in red; 5,000 cells/g/mouse) were simultaneously infused into a recipient mouse. Circulating MPs and cells were detected in the microcirculation before injury (second from left). Note that no fluorescent signal was detected before infusion of MPs and cells (left). The experiment was independently performed three times in three mice.

Endogenous cancer-derived MPs accumulate at the site of thrombus formation in vivo

To determine if cancer cells and/or MPs shed during tumor growth could participate and influence thrombus formation in vivo, an ectopic tumor was induced by injection of Panc02 cells labeled with quantum dots (Qdots). Using this compound, we were able to detect fluorescence in vitro for more than a week in cultured cells and in MPs shed from the cells (unpublished data). 1 wk after injection of Qdot-labeled cells, $FeCl_3$ injury was administered to the mesentery of the mouse. The presence of Panc02 cells and/or MPs at the site of injection, in the circulation, and at the site of injury was followed by in vivo imaging. As expected, when Qdots alone were injected into mice, a fluorescent signal was detected 1 wk later only at the site of injection. In contrast, Qdot-labeled cells and/or MPs were detected at the site of injection and in the circulation, and also accumulated at the site of injury (Fig. 6 A). These results indicate that in mice developing ectopic tumors, cancer cells and/or cancer-derived MPs may reach the bloodstream and accumulate at the site of injury, suggesting that these MPs may influence the kinetics of thrombus growth. To discriminate between Panc02 cells and endogenous Panc02-derived MPs (produced by the tumor in contrast with MPs prepared in vitro and infused into the bloodstream), we stably transfected Panc02 cells with the pEGFP-N1 vector encoding GFP (Fig. 6 B). 5 wk after subcutaneous injection of Panc02 cells overexpressing GFP, the presence and accumulation of a fluorescent signal before and after injury induced by a dye laser (Dubois et al., 2006a; Dubois et al., 2007) were detected in the cremaster microcirculation using the intravital microscope. Particles were observed, ranging in size from 0.4 (the minimum size we were able to detect using our system) to 1 μm (the maximum size measured for detected particles), that were likely endogenous MPs circulating in the blood circulation (Fig. 6 C) and accumulating at the site of injury in both venules (Fig. 6 D, left) and arterioles (Fig. 6 D, right). Together with our previous results showing that Panc02-derived MPs but not Panc02 cells accumulate at the site of injury, we conclude that Panc02-derived MPs shed from a growing tumor circulate in the bloodstream and participate in thrombus formation in mice.

Endogenous cancer-derived MPs accumulate at the site of injury by binding to P-selectin and accelerate thrombus growth in a TF-dependent pathway

The thrombotic effects of cancer cell–derived MPs on tail bleeding time (Fig. 7 A) and time to occlusion of arterioles (Fig. 7 B) and venules (Fig. 7 C) were significantly decreased

Table I. Number and cellular origins of MPs ($\times 10^6$/liter^{-1} plasma) in healthy and cancer mice

MP origins	Controls (n = 8)	Pancreatic cancer (n = 8)	Lung cancer (n = 7)	p-value[a]	p-value[b]
	$\times 10^6$/liter^{-1} plasma	*$\times 10^6$/liter^{-1} plasma*	*$\times 10^6$/liter^{-1} plasma*		
Total (annexin V$^+$)					
Median	8,951	9,383	10,018	0.024	0.047
Range	5,994–14,714	5,536–14,794	5,048–16,442		
Platelet (CD41$^+$)					
Median	2,294	3096	3,024	0.035	0.014
Range	1,724–3,216	1,636–5,476	770–8,784		
Erythrocyte (TER 119$^+$)					
Median	1,410	694	828	0.149	0.242
Range	250–4,672	288–2,712	478–2,480		
Leukocyte (CD45$^+$)					
Median	346	251	722	0.209	0.424
Range	74–1,032	130–888	68–2,206		
Endothelial cell (CD31$^+$CD41$^-$)					
Median	135	275	164	0.001	0.014
Range	108–330	150–336	92–296		
MUC-1$^+$					
Median	117	1089	1,492	0.003	0.003
Range	0–7,424	0–15,468	98–4,786		
CA19.9$^+$					
Median	0	264	127	0.001	0.003
Range	0	0–6,852	0–2,428 (n = 6)		
Annexin V$^+$ PSGL-1$^+$					
Median	146	293	234	0.004	0.006
Range	76–376	74–522	134–550		

[a]Differences between mice developing a pancreatic cancer and healthy mice.
[b]Differences between mice developing a lung cancer and healthy mice.

when proteins at the surface of MPs were stripped by trypsin before infusion into the recipient mouse. Cancer cells and MPs express TF on their surfaces (Fig. 1). To determine whether TF was present in a decrypted (active) form on the surface of cancer cells and MPs, the activity of TF present on SOJ-6, Panc02, and LLC1 cells, as well as MPs, was determined.

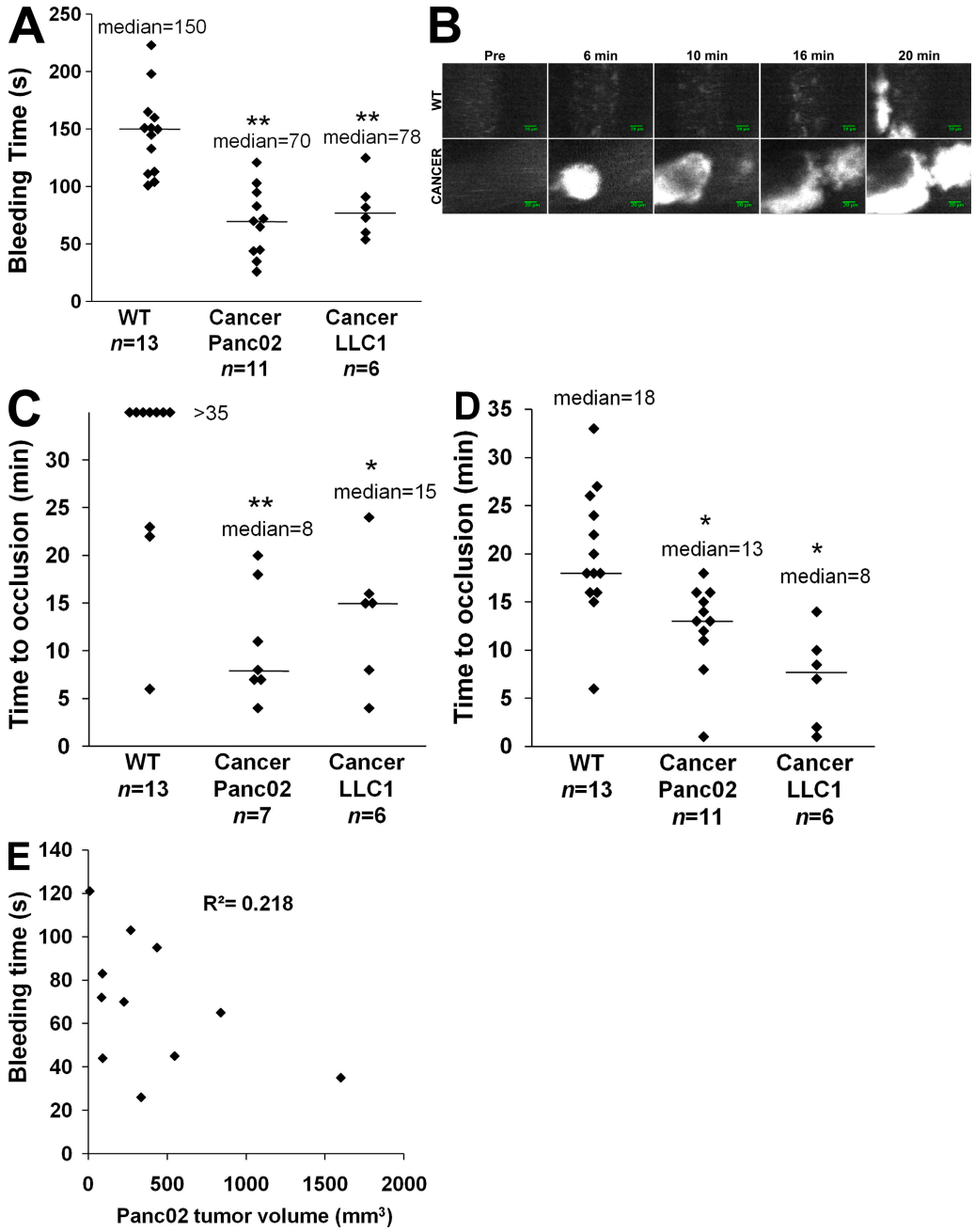

Figure 5. Characterization of a thrombotic state in mice developing tumors. Kinetics of thrombosis in wild-type mice or in mice developing Panc02-derived (Cancer Panc02) or LLC1-derived (Cancer LLC1) tumors. (A) Bleeding times were determined in wild-type mice (n = 13 mice), mice developing a Panc02 tumor (n = 11 mice), or mice developing an LLC1 tumor (n = 6 mice). (B) Thrombus formation was studied after infusion of Alexa Fluor 660–conjugated anti-CD41 Fab fragment and Syto 62 in wild-type mice and in mice developing tumors. Injury was induced in mesenteric vessels by topical application of 10% $FeCl_3$ for 5 min. Representative fluorescence images depicting the kinetics of thrombus formation of labeled platelet accumulation (white) on mesenteric arterioles (Pre, before injury). (C and D) Time to vessel occlusion reported in minutes for mesenteric arterioles (n = 13, 7, and 6 thrombi for WT, Cancer Panc02, and Cancer LLC1, respectively; C) and venules (n = 13, 11, and 6 thrombi for WT, Cancer Panc02, and Cancer LLC1, respectively; D). One injury was performed per mouse. (E) Bleeding times (in seconds) in function of the tumor volume (in mm^3) in Panc02 tumor–bearing mice (n = 11). The linear coefficient of determination value is represented by R^2. Horizontal bars in A, C, and D indicate median values. Experiments were independently performed at least six times (A–D) and 11 times (E). **, $P < 0.01$; *, $P < 0.05$.

As previously described by others (Milsom et al., 2007; Pawlinski and Mackman, 2008), we observed that cancer cells express active TF, demonstrating activity ranging from 7×10^{-4} pmol/cell for the two mouse cancer cell lines tested to 17×10^{-4} pmol/cell for human SOJ-6 cancer cells (Fig. 7 D). All MPs studied expressed similar concentrations of active TF (between 2.3×10^{-4} and 4.3×10^{-4} pmol/MP). We then determined the activity of TF as a ratio of TF concentration to surface area to control for the difference in size between a cancer cell (diameter = 20 μm) and an MP (diameter = 1 μm). Results obtained show that the density of active TF is increased >100-fold in MPs as compared with cancer cells. (Fig. 7 D). These cancer cell–derived MPs were able to activate platelets and to induce platelet aggregation and formation of a fibrin mesh after addition of platelet-poor plasma (PPP) to a washed platelet preparation (Fig. 7 E). This effect was slightly inhibited when a fibrinogen-deficient plasma was added to the platelet preparation and was abolished by using a factor VII–depleted PPP (Fig. 7 E). These data demonstrate that MPs activate and aggregate platelets via a TF-dependent pathway in vitro.

To determine whether endogenous MPs arising from cancer cells accumulate in the thrombus growth via an interaction between PSGL-1 and P-selectin, the accumulation of endogenous Panc02-derived MPs was compared at the site of injury before and after infusion of a blocking P-selectin monoclonal antibody, as previously described (Falati et al., 2003; Vandendries et al., 2007). Although accumulation of endogenous MPs was observed after laser- or $FeCl_3$-induced injury (Fig. 8 A, left) to the mesentery, no signal corresponding to endogenous cancer cell–derived MPs bound to a thrombus was detected upon infusion of the P-selectin antibody (Fig. 8 A, right). The same results were observed when exogenous DiD-labeled cancer cell–derived MPs were infused into the circulation in the presence of blocking antibody (unpublished data). We conclude that cancer cell–derived MPs accumulate at the site of thrombus formation via interactions between the PSGL-1 expressed at their surface and P-selectin expressed on activated platelets and endothelial cells. Furthermore, the median times to occlusion in arterioles (Fig. 8 B) and venules (Fig. 8 C) were significantly higher when cancer cell–derived MPs were infused in the presence of blocking P-selectin antibody than when they were infused alone ($P < 0.05$). These results were confirmed by determining the tail bleeding time, which was significantly higher in the presence of P-selectin ($P < 0.01$; Fig. 8 D). Collectively, our results indicate that tumor-shed MPs reach the bloodstream, accumulate at the site of injury in a P-selectin-dependent manner, and accelerate thrombus growth mainly via a TF-dependent pathway.

DISCUSSION

In the present paper, we studied the role of cancer cell–derived MPs in thrombus formation. To characterize the thrombotic/coagulation state in vivo, we measured the kinetics of thrombus formation after a chemical- or laser-induced injury. We also compared the tail bleeding time of healthy mice, mice developing tumors, and mice after infusion of cancer cells and MPs. Our results indicate that pancreatic and lung cancer cells are able to shed MPs expressing TF and PSGL-1 on their surface. In vivo, in a mouse model of cancer, these MPs circulate in the blood, accumulate at the site of injury in a P-selectin–dependent manner, and may participate in

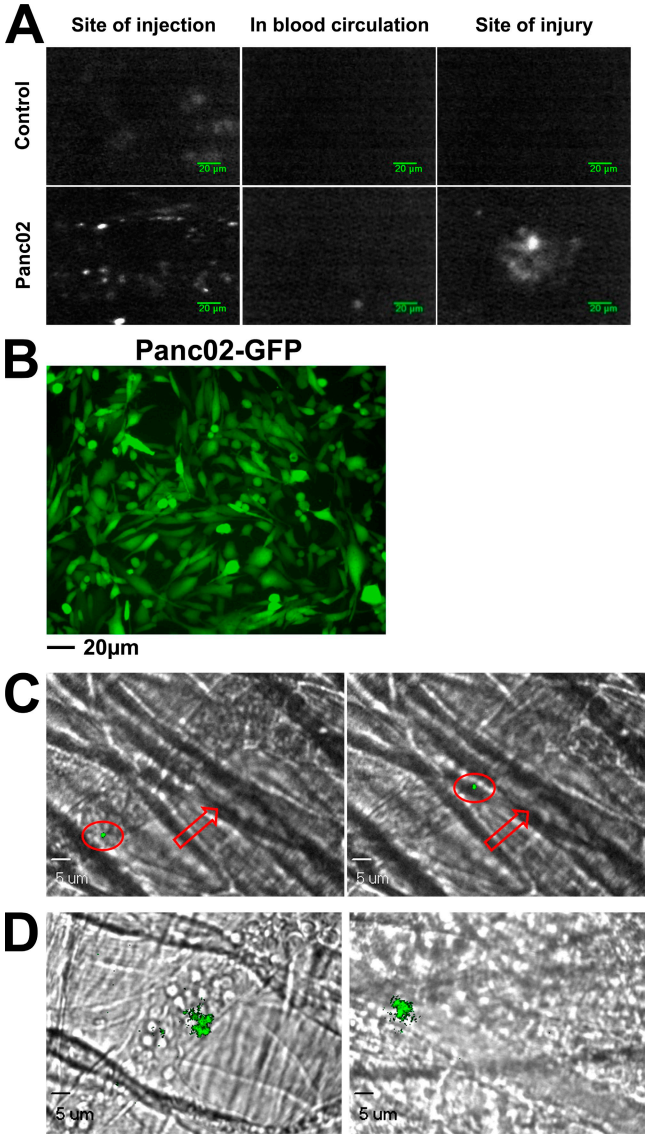

Figure 6. Endogenous cancer cell–derived MPs accumulate at the site of thrombus formation in vivo. (A) Qdot-labeled Panc02 cells (2×10^6 cells) or Qdots alone (Control) were injected subcutaneously into the right flank of a mouse. 1 wk later, fluorescent signals were detected at the site of injection (left), and in the mesentery before (middle panel) and after (right) $FeCl_3$-induced injury. (B) Fluorescence microscopy of Panc02 cells overexpressing GFP before subcutaneous injection into wild-type mice. (C and D) 2×10^5 Panc02 cells overexpressing GFP were injected subcutaneously into the right flank of a mouse. 5 wk later, the cremaster was isolated and fluorescent circulating GFP-labeled MPs were detected in the blood microcirculation (red arrow, direction of the blood flow; red circle, GFP microparticle; C) and accumulating at the site of injury in venules (D, left) and arterioles (D, right). All images are representative of three independent experiments observed for nine thrombi formed in three mice.

the generation of thrombin, likely via the expression of active TF at their surface. The presence of MPs is necessary for the formation of a thrombotic state in vivo. Finally, our results show that cancer cells do not accumulate at the site of injury and do not accelerate the kinetics of thrombosis in our model. To our knowledge, this is the first study to use imaging of endogenous cancer cell–derived MPs and cancer cells to characterize their respective roles in the kinetics of thrombus formation in vivo.

Among the different proteins able to activate and aggregate platelets while simultaneously favoring the process of metastasis, TF expressed on cancer cells has been suggested to play a key role in the development of a cancer-associated thrombotic state (Riewald and Ruf, 2001; Haas et al., 2006;

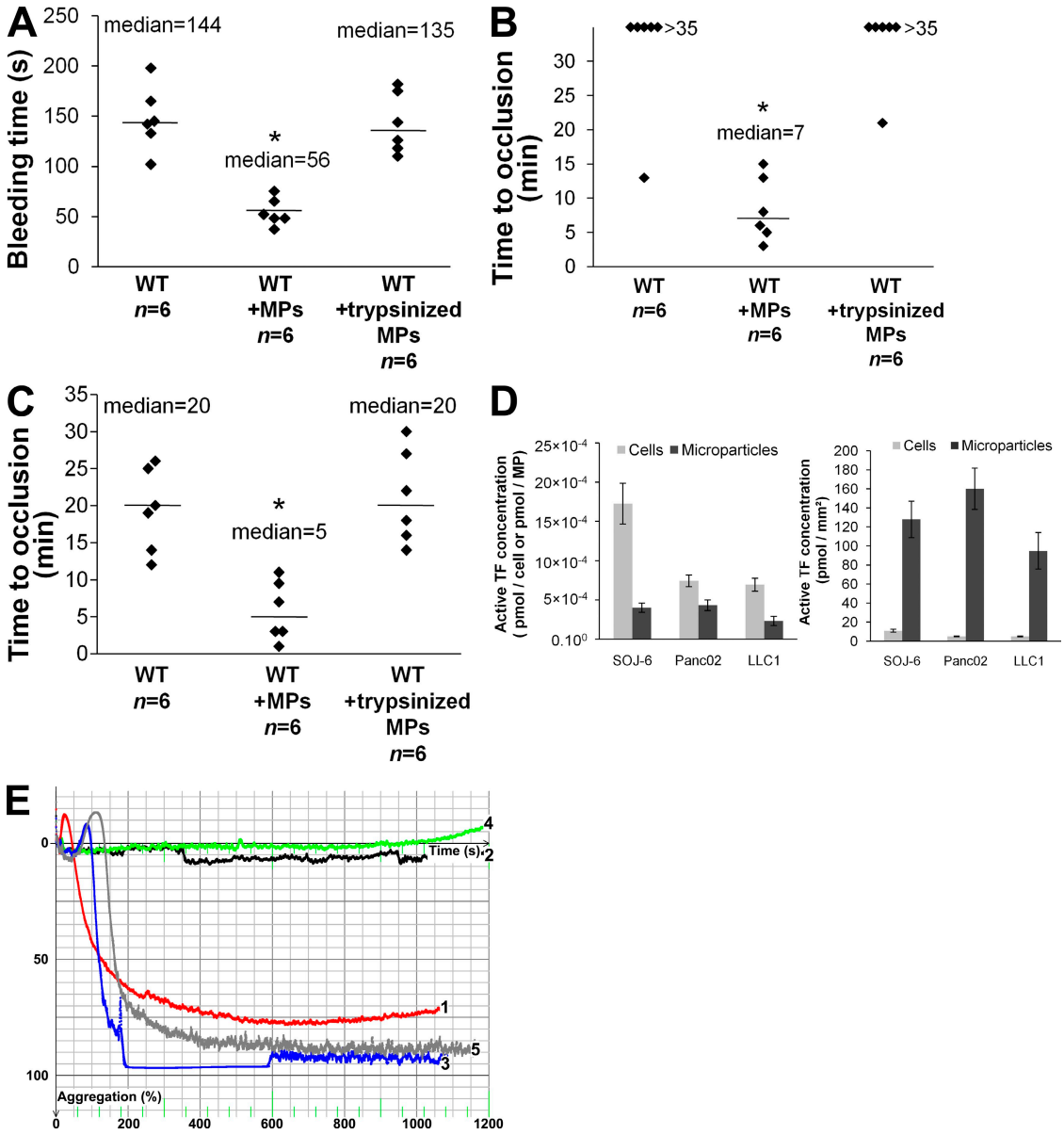

Figure 7. Endogenous cancer-derived MPs accelerate thrombus growth through a TF-dependent pathway. (A–C) Kinetics of thrombosis in mice perfused with control Panc02 MPs or trypsinized Panc02 MPs (18,000 MPs/g/mouse) compared with wild-type mice. (A) Bleeding time of wild-type mice and of mice perfused with control MPs (WT+MPs) or trypsinized MPs (WT+trypsinized MPs; $n = 6$ mice for each group). Time to vessel occlusion reported in minutes for mesenteric arterioles (B) and venules (C; $n = 6$ thrombi in six mice for each group). Injury of the mesenteric vessels was induced by topical application of 10% $FeCl_3$ for 5 min. Horizontal bars indicate median values. **, $P < 0.01$; *, $P < 0.05$. (D) Measurement of TF activity on the surface of cancer cells and MPs in pmol/cell^{-1} and pmol/MP^{-1} (left) or in pmol/mm^2 (right), reported as the mean ± SD. (E) Aggregation of 2.5×10^8 human washed platelets/ml induced by addition of thrombin (Curve 1, red), SOJ-6 MPs (1 µg of MP-associated proteins/ml) in the absence (Curve 2, black) or presence of 5% vol/vol (final) of PPP (Curve 3, blue), factor VII–depleted PPP (Curve 4, green), or fibrinogen-deficient PPP (Curve 5, gray). Experiments were independently performed six times (A–C) and three times (D and E).

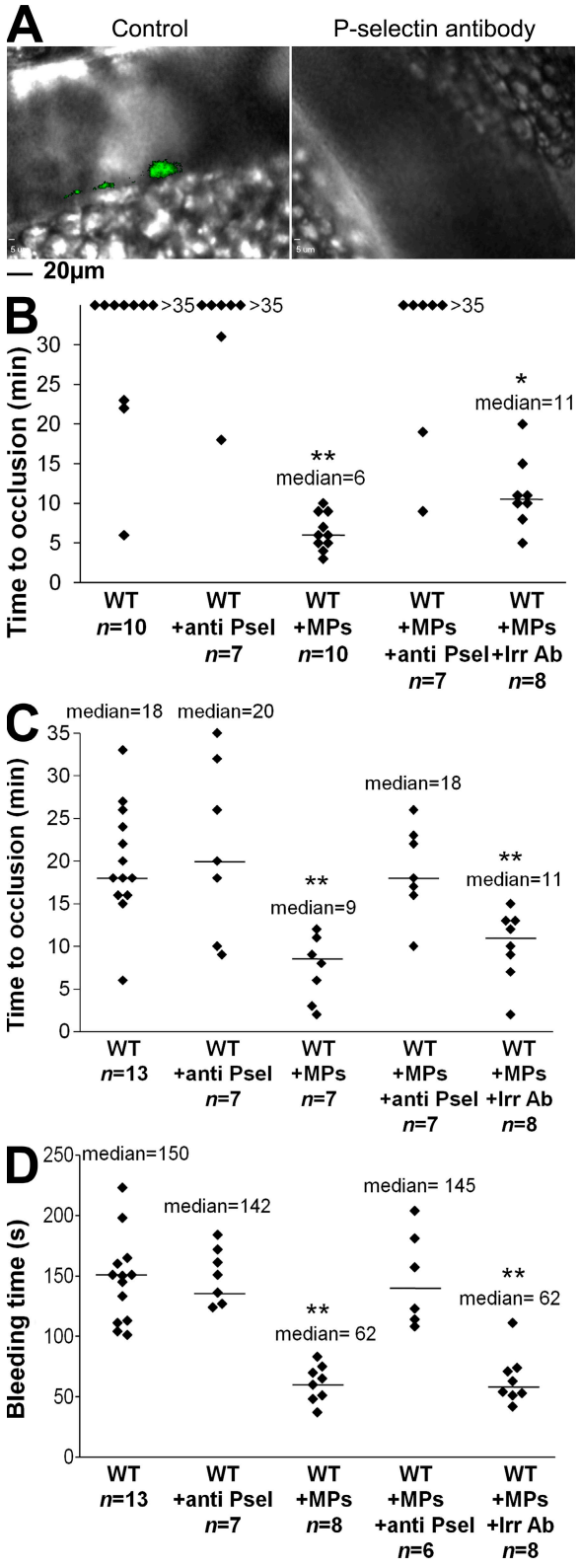

Figure 8. Endogenous cancer-derived MPs accelerate thrombus formation in a P-selectin–dependent manner. (A) 2×10^5 Panc02 cells overexpressing GFP were injected subcutaneously into the right flank of a mouse. 5 wk later, chemical injury of the mesentery was induced, and fluorescence was detected in the absence (left, Control) or presence of circulating P-selectin blocking antibody (right, P-selectin antibody; $n = 6$ thrombi in three mice). (B–D). Kinetics of thrombosis in wild-type mice, wild-type mice infused with Panc02 MPs (WT+MPs, 0.2 µg of MP-associated proteins/g/mouse), or with Panc02 MPs plus 2 µg/g/mouse of anti P-selectin blocking antibody (WT+MPs+anti P-sel). Controls were performed by infusion of anti–P-selectin antibody into wild-type mice (WT+anti P-sel) or by infusing an irrelevant antibody into wild-type mice perfused with MPs (WT+MPs+Irr Ab). Injury of the mesenteric vessels was chemically induced, and the time to vessel occlusion for arterioles ($n = 10$ for WT, $n = 7$ for WT+anti Psel, $n = 10$ for WT+MPs, $n = 7$ for WT+MPs+anti Psel, and $n = 8$ for WT+MPs+Irr Ab; B) and veinules ($n = 13$ for WT, $n = 7$ for WT+anti Psel, $n = 7$ for WT+MPs, $n = 7$ for WT+MPs+anti Psel, and $n = 8$ for WT+MPs+Irr Ab; C) was measured. (D) Bleeding times were determined for all conditions studied ($n = 13$ for WT, $n = 7$ for WT+anti Psel, $n = 8$ for WT+MPs, $n = 6$ for WT+MPs+Anti Psel, and $n = 8$ for WT+MPs+Irr Ab). One thrombus was performed per mouse. Horizontal bars designate median values. Experiments were independently performed three times (A) and at least seven times (B–D). **, $P < 0.01$; *, $P < 0.05$.

Versteeg et al., 2008). However, no direct correlation could be established between the presence of TF on cancer cells and the development of thrombosis complications associated with cancer (Furie and Furie, 2006), suggesting that other important mechanisms may link cancer and thrombosis. Recently, various reports have shown that the number of circulating MPs is increased in patients developing different types of cancers known to be associated with a thrombotic state (Kim et al., 2003; Del Conde et al., 2007; Zwicker et al., 2007). These observations suggest that MPs may play a key role in the development of the thrombotic complications associated with cancer. Our results indicate that MPs derived from cancer cells enhance thrombus formation. The presence of PSGL-1 targets MPs to sites of thrombosis, whereas active TF actively participates in the formation of the thrombus by generating thrombin and fibrin. Two recent reports have shown, in mice models, a direct correlation between the size of a tumor and the level of TF present in cell-free plasma (Yu et al., 2005; Davila et al., 2008). We did not observe such correlation when comparing the bleeding time associated with the volume of the tumors (Fig. 5 E). Indeed, even relatively small tumors are sufficient enough to strongly diminish the tail bleeding time and the occlusion time in our model. These results confirm that the presence in the bloodstream of few tumor-derived MPs is sufficient enough to induce a thrombotic state in mice. Last, in the two papers, authors have not discriminated the origin of circulating TF that may come from platelets or monocyte-derived MPs. Other studies have previously shown that such MPs may originate from platelets (Hron et al., 2007; Tesselaar et al., 2007). In this study, we observed that the quantities of circulating platelet-, endothelial cell–, and cancer cell–derived MPs are increased in mice developing tumors compared with healthy mice. With the knowledge that platelets release MPs only when they aggregate (Piccin et al., 2007), it not surprising that the amount of circulating MPs derived from platelets increases when patients/mice develop a thrombotic state. Indeed, this pathological

state leads to the activation and aggregation of platelets, either directly via cancer cells or indirectly via production of thrombin by TF. Therefore, it is likely that platelet-derived MPs are a consequence of thrombotic complications and do not cause the development of this phenotype. However, platelet-derived MPs, when present in the blood, may also participate in the stability of a thrombotic state associated with cancer. Endothelial cells activated by tumoral MPs may provide a supplementary procoagulant surface by TF exposure. Although several reports have shown that TF is expressed on cancer cells, there is conflicting evidence as to the presence of this factor at the surface of platelets and their MPs (Furie and Furie, 2006). To our knowledge, this is the first paper to demonstrate an increase in circulating endothelial cell–derived MPs in association with cancer. However, previous publications have shown that the level of endothelial cell–derived MPs is increased in inflammatory-related diseases (Combes et al., 1999; Chamouard et al., 2005). These MPs, by expressing proteins such as metalloproteases, urokinase plasminogen activator, and urokinase plasminogen activator receptor (Lacroix et al., 2007), may potentially take part in and amplify the processes of inflammation, angiogenesis, and fibrinolysis. Further experiments are needed to determine the actual role of platelet-derived MPs in concert with cancer cell– and endothelial cell–derived MPs.

When cancer cells and cancer cell–derived MPs were infused into the circulation of a living mouse, only MPs were observed to accumulate at the site of a laser- or chemical-induced injury, suggesting that cancer cells may not participate in thrombus formation. These cells were not eliminated from the blood, because we were able to detect them circulating in the vessels (Fig. 4 C, before injury). This result was confirmed by our data showing that injection of cancer cells did not influence either the kinetics of thrombus formation or bleeding times. Our results are consistent with previous observations showing that monocyte-derived MPs, but not their parent cells, may indeed interact with a growing thrombus (Falati et al., 2003). Although circulating cancer cells did not bind to the site of injury, they may interact with the endothelium at sites of premetastatic niches to form sites of metastasis (Kaplan et al., 2006). Different hypotheses may explain why MPs and not their parental cells bind to a growing thrombus. It is possible that this interaction occurs via the negative phospholipid moieties commonly expressed on the surface of MPs. Furthermore, the quantity and density of binding partners present, such as PSGL-1, may be more important for MPs than for their parent cells. This point is illustrated by our results showing that even if the activity of cell TF was greater than that of the MP, when the results were reported per surface unit, the activity of TF was >100-fold higher in MPs than in cells. This result may also explain why the cells were not thrombogenic compared with MPs. In our conditions, Panc02-derived MPs have a more dramatic effect on thrombosis in arterioles compared with venules, whereas LLC1-derived MPs have the opposite effect. This tendency may be caused, at least partially, by the levels of active TF expressed by Panc02- and LLC1-derived MPs. Indeed, activation of the coagulation cascade resulting in thrombin generation is known to play a more important role in thrombus formation induced in arteries than in veins.

We demonstrated that PSGL-1 is present on the surface of MPs and showed that injection of a P-selectin blocking antibody prevents the accumulation of MPs at the site of injury and reduces thrombus formation. The P-selectin–PSGL-1 axis has previously been described as being involved in the binding of MPs to platelets. Indeed, Falati et al. (2003) have previously shown that exogenous monocyte-derived MPs express PSGL-1 and bind to a growing thrombus in a P-selectin–dependent manner in a laser injury model. We determined that inhibition of P-selectin did not affect time to occlusion in the $FeCl_3$ model in healthy mice, showing that accumulation of monocyte-derived MPs by the P-selectin–PSGL-1 axis may have a minor implication when cancer-derived MPs are not involved in thrombus formation after a $FeCl_3$-induced injury. Our results identify P-selectin as a potentially good pharmaceutical target for the prevention of thrombosis associated with cancer, and may also explain why heparin, which binds to and blocks selectin, is much more effective than warfarin, a vitamin K antagonist, in preventing thrombosis in patients suffering from Trousseau's syndrome (Del Conde et al., 2007). MPs also express negatively charged phospholipids on their surface that may participate with TF in activation of the coagulation cascade. However, based on our results, the activity of TF seems to be critical for the generation of thrombin. Indeed, we found that (a) in vitro TF activity per surface unit is 100-fold more important in MPs than in their parental cells (Fig. 7 D), (b) the use of factor VII–deficient plasma abolishes the effect of MPs on platelet aggregation and the formation of a fibrin mesh (Fig. 7 E), and (c) in vivo hydrolysis of the surface proteins but not the negatively charged phospholipids present on MPs completely abrogated their effect on the kinetics of thrombosis (Fig. 7, A–C). Based on our results, we propose a two-step mechanism to describe the involvement of cancer cell–derived MPs in thrombosis. First, MPs bind to the site of injury by interactions between PSGL-1 and P-selectin present on activated platelets and endothelial cells. Second, MPs affect thrombus formation, likely via the expression of active TF on their surface. Other proteins and lipids may also be of importance in this process. Among the different proteins expressed by cancer cell–derived MPs, fetoacinar pancreatic protein and fibronectin were identified (unpublished data; Ni et al., 2003). Both of these may play an important role in thrombus formation. Fetoacinar pancreatic protein, an onco-isoform of bile salt–dependent lipase, increases the kinetics of thrombus formation by binding to CXCR4 on the surface of activated platelets (Panicot-Dubois et al., 2007). Overall, our data provide a new molecular basis for establishing relationships between cancer and thrombosis, and may facilitate the development of new pharmaceutical drugs designed to prevent thrombosis and metastasis in patients suffering from cancer.

MATERIALS AND METHODS

Mice. Wild-type C57BL/6J mice were obtained from Janvier. All animal care and experimental procedures were performed as recommended by the European Community guidelines and approved by the local ethical committee of the Université de la Méditerranée and the French Ministry of Agriculture (agreement no. 13.382).

Antibodies and reagents. Rat monoclonal anti–mouse CD41 antibody (clone MWReg30) was obtained from Emfret. Fab fragments for the anti-CD41 antibody were generated by using the immunopure Fab preparation kit from Thermo Fisher Scientific, and then conjugated to Alexa Fluor 660. Human α-thrombin, factor VII–deficient plasma, and sheep anti–human TF were obtained from Biopep. Rabbit anti–mouse TF was purchased from American Diagnostica Inc. PE rat anti–mouse CD41 (clone MWReg30), PE rat anti–mouse CD45 (clone 30-F11), PE rat anti–mouse CD31 (clone MEC 13.3), PE rat anti–mouse TER-119 (clone TER-119), PE rat anti–mouse PSGL-1, blocking rat monoclonal anti–mouse P-selectin (clone RB40.34), and rat monoclonal anti–mouse PSGL-1 (clone 4RA10) antibodies, and FITC–annexin V, PE–annexin V, and PE rat and mouse isotype controls were obtained from BD. Monoclonal anti-CA19.9 and anti–MUC-1–core glycoprotein antibodies were purchased from Novocastra Laboratories and were conjugated in house to Alexa Fluor 488. Irrelevant rat immunoglobulins were purchased from BD and SouthernBiotech. Peroxydase-conjugated donkey anti–rat, donkey anti–rat–Alexa Fluor 488, donkey anti–sheep–Alexa Fluor 488, and donkey anti–rabbit–Alexa Fluor 594 antibodies; Vybrant DiD and DiO cell-labeling solutions; the Qtracker 705 cell labeling kit; Alexa Fluor 594 and Alexa Fluor 660 antibody-labeling kits; Syto 62, Lipofectamine 2000, PLUS reagent, RPMI 1640, DMEM, and OptiMEM media; and penicillin, streptomycin, L-glutamine, trypsin-EDTA, nonenzymatic cell dissociation solution, and fungizone were obtained from Invitrogen. Megamix beads were purchased from BioCytex. Prostaglandin I_2 was obtained from EMD. BSA, apyrase grade VI, Gly-Pro-Arg-Pro, and $FeCl_3$ were purchased from Sigma-Aldrich. pEGFP-N1 vector was obtained from Clontech Laboratories, Inc. Tirofiban (Aggrastat) was purchased from Iroko Pharmaceuticals.

Cell lines and culture conditions. One cell line from human pancreatic adenocarcinomas (SOJ-6; Fujii et al., 1990), and two cell lines from a mouse pancreatic adenocarcinoma (Panc02) and a Lewis lung carcinoma (LLC1) were studied. The Panc02 cell line has been established and described by Corbett et al. (1984). In brief, it is derived from a pancreatic ductal adenocarcinoma induced by implantation of cotton thread–carrying 3-methylcholanthrene into the pancreas tissue of a C57BL/6 mouse. The LLC1 cell line has been established and described by Bertram and Janik (1980) and was obtained from the American Type Culture Collection. It is derived from a Lewis lung carcinoma of a C57BL mouse strain. The Panc02 cell line was provided by E. Beraud (Institut National de la Santé et de la Recherche Médicale [INSERM] UMR911, Marseille, France). L929 mouse fibroblasts and J774 mouse macrophages were provided by F. Levy (INSERM UMR608, Marseille, France). SOJ-6, LLC1, L929, and J774 cells were grown in DMEM medium, and Panc02 cells were grown in RPMI 1640 medium. Media were supplemented with 10% FCS, 2 mM L-glutamine, 100 U/ml penicillin, 100 μg/ml streptomycin, and 0.1% fungizone. Cells were grown at 37°C in a humidified atmosphere with 5% CO_2.

Transfection. Panc02 cells were stably transfected with the pEGFP-N1 plasmid using Lipofectamine 2000 and PLUS reagent according to the manufacturer's recommendations. Cells were cloned as previously described (Panicot-Dubois et al., 2004).

Isolation of MPs. The isolation of MPs was adapted from Berckmans et al. (2001). In brief, cells at 80% of confluency were incubated for 15 h in OptiMEM medium. MP-rich medium was centrifuged at 1,500 *g* to eliminate cellular debris and ultracentrifuged at 20,000 *g* to isolate MPs. The final pellet containing MPs was resuspended in 0.5 ml PBS. Mice MPs were isolated as previously described (Dignat-George, 2006). L929 and J774 cells were activated with 10 ng/ml TNF-α before MP isolation. Concentrations of MPs were determined by protein quantification using the bicinchoninic acid assay (Thermo Fisher Scientific).

PAGE and Western blotting. SDS-PAGE performed on gels of polyacrylamide (7.5% acrylamide in the presence of 0.1% sodium dodecyl sulfate) and Western blotting were performed as previously described (Panicot-Dubois et al., 2007).

Flow cytometry. Platelet-free plasma (PFP) samples were prepared as previously described (Sabatier et al., 2002) using serial centrifugations and stored at −80°C until use. For MP labeling, 30 μl of freshly thawed PFP or of the MP suspension was incubated for 30 min with 10 μl FITC–annexin V or PE–anti–mouse monoclonal antibodies (30 μg/ml anti-CD41, 40 μg/ml anti–TER-119, 40 μg/ml anti-CD45, 40 μg/ml anti-CD31, or 50 μg/ml anti–PSGL-1). Concentration-matched PE-isotype antibodies (IgG1, clone R3-34; IgG2a, clone R35-95; IgG2b, clone A95-1) or annexin V–FITC with phosphate-buffered saline without calcium were used as control. Analyses were performed on a flow cytometer (Cytomics FC500; Beckman Coulter) using a Megamix bead–calibrated protocol (BioCytex), as previously described (Robert et al., 2009). Flow-Count fluorospheres (Beckman Coulter) were added to each sample to express MP counts as absolute numbers.

Fluorescence microscopy. Cells were grown up to 80% confluence on an 8-chamber glass slide system (Thermo Fisher Scientific), washed with PBS, and fixed for 30 min at 4°C in PBS containing 2% paraformaldehyde. Once fixed, cells were blocked for 1 h at 4°C with 1% BSA in PBS buffer. Cells were then incubated at 4°C with the appropriate dilution of antibodies, followed by incubation with an Alexa Fluor 488– or Alexa Fluor 594–conjugated secondary antibody. Between each step, cells were exhaustively rinsed with PBS and were observed on a microscope (Axiovert 200; Carl Zeiss, Inc.).

TF activity assays. A chromogenic assay (Actichrome TF; American Diagnostica Inc.) was used to analyze TF activity. TF activity was measured in cell or MP suspension according to the manufacturer's instructions. Cells or MPs were incubated in the presence of factors VIIa and X. The reagents were incubated at 37°C for complex formation to convert factor X to factor Xa, and the amount of Xa generated was measured by its ability to cleave a chromogenic substrate, spectrozyme Xa. Absorbance was read at 405 nm with a microplate reader (MR5000; Dynatech). TF concentration was determined by interpolation of a standard curve obtained from different amounts of lipidated TF standards. For TF activity measurement in mouse plasma, a TF/TF pathway inhibitor–depleted plasma was added to the reaction mixture of lipidated TF standards, and ΔA405–490 was measured to calculate TF concentration.

Platelet aggregation studies. Washed platelets were obtained as previously described (Dubois et al., 2004). 2.5×10^8 washed platelets/ml were stirred at 37°C for 10 min in 2 × 4-channel aggregometers (Apact 4004; LABiTec). Positive controls were performed in the presence of 1 U/ml thrombin. The extent of platelet aggregation was defined as the percent change in optical density (Dubois et al., 2007).

MP half-life. The carotid arteries and jugular veins of 8-wk-old mice were cannulated. DiO-labeled MPs were infused in the bloodstream via the jugular veins. Blood samples were collected in sodium citrate (3.2%, 1:2 vol/vol) via the carotid artery catheter before MP injection and 5, 15, 30, 45, and 60 min after injection.

Induction of ectopic tumor. For all in vivo experiments, tumor cells in the exponential growth phase were briefly exposed to nonenzymatic cell dissociation buffer to dislodge the cells. They were next carefully washed, resuspended in PBS, and diluted to the desired cell number/inoculum. 3-wk-old C57BL/6 mice were injected subcutaneously into the right flank with 2×10^5 Panc02 cells, 2×10^5 LLC1 cells, 2×10^6 Panc02-labeled cells, or with

PBS alone for control mice. Cells were labeled with Qdots (Qtraker 705), DiD, or DiO according to the manufacturer's instructions (Invitrogen).

Intravital microscopy. Mice were anesthetized with an intraperitoneal injection of 100 mg/kg ketamine and 12.5 mg/kg Xylazine (Bayer). The jugular vein was cannulated to maintain anesthesia by injection of 50 mg/kg pentobarbital injection and to infuse antibodies, cells, and MPs as needed. The trachea was intubated to facilitate spontaneous respiration by the mouse, and a thermocontrolled blanket maintained the mouse at 37°C. Cremaster and mesentery preparations were performed as previously described by Dubois et al. (2007). Intravital videomicroscopy was performed as previously described (Dubois et al., 2007; Panicot-Dubois et al., 2007). Data were obtained using a microscope (BX61WI; Olympus) with a 60 × 0.9 or a 20 × 0.5 NA water immersion objective. Alternatively, a fibered fluorescence microscopy imaging system (Cellvizio; Mauna Kea Technologies) was used to image platelets. The optical probe used in this study has a tip diameter of 4.2 mm (MiniO/100; Mauna Kea Technologies), providing images below the surface of biological tissue and at a depth 100 ± 5 µm, with a lateral resolution of 1.8 µm.

$FeCl_3$-induced injury. The $FeCl_3$-induced model of thrombosis has been shown to cause substantial damage to the endothelium and exposure of underlying collagen (Dubois et al., 2006b). Vessel injuries were generated by using a 1 × 2–mm filter paper soaked with a 10% $FeCl_3$ solution and placed over the vessel for 5 min, as previously described (Dubois et al., 2006b). Platelet accumulation at the site of injury was detected by infusion in blood circulation of 250 ng/g/mouse of anti-CD41 Fab fragment coupled with Alexa Fluor 660 for 35 min or until blood flow cessation lasted for >10 s (occlusion). Typically, one venous and one arterial injury were performed per mouse.

Laser-induced injury. Vessel-wall injuries were induced with a nitrogen dye laser (Micropoint; Photonics Instruments) focused through the microscope objective, parfocal with the focal plane and aimed at the vessel wall, as previously described (Dubois et al., 2006b; Dubois et al., 2007). Typically, one or two pulses were required to induce vessel wall injury.

Tail bleeding time. Tail bleeding times were performed as previously described on anesthetized 8-wk-old mice (Dubois et al., 2007).

Statistics. Significance was determined by a paired two-tailed Student's *t* test for the in vitro experiments and by Wilcoxon's rank-sum test for the in vivo experiments. The difference was considered significant at $P < 0.05$.

Online supplemental material. Fig. S1 shows the box plot distribution of $CD31^+CD41^-$ MPs and $TER119^+$ MPs in healthy and tumor-bearing mice (data are from Table I). Online supplemental material is available at http://www.jem.org/cgi/content/full/jem.20082297/DC1.

The authors are indebted to L. Arnaud for the quantification of MPs. The authors are grateful to J. Varin, J. Courageot, and C. Prévot for expert technical assistance, and to M.-C. Alessi for the use of the aggregometers. The authors thank P.-A. Dancer, B. Brisson, J. Rebouillat, A. Hembury, and Mauna Kea Technologies for the use of the Cellvizio fibered fluorescence microscopy imaging system.

This work was supported by institutional funding from INSERM and Aix-Marseille Université. This work was supported by the Association pour la Recherche sur le Cancer (grant ARC-1038 to C. Dubois).

The authors have no conflicting financial interests.

Submitted: 14 October 2008
Accepted: 17 July 2009

REFERENCES

Abid Hussein, M.N., E.W. Meesters, N. Osmanovic, F.P. Romijn, R. Nieuwland, and A. Sturk. 2003. Antigenic characterization of endothelial cell-derived microparticles and their detection ex vivo. *J. Thromb. Haemost.* 1:2434–2443.

Berckmans, R.J., R. Neiuwland, A.N. Böing, F.P. Romijn, C.E. Hack, and A. Sturk. 2001. Cell-derived microparticles circulate in healthy humans and support low grade thrombin generation. *Thromb. Haemost.* 85:639–646.

Bertram, J.S., and P. Janik. 1980. Establishment of a cloned line of Lewis Lung Carcinoma cells adapted to cell culture. *Cancer Lett.* 11:63–73.

Blom, J.W., S. Osanto, and F.R. Rosendaal. 2006a. High risk of venous thrombosis in patients with pancreatic cancer: a cohort study of 202 patients. *Eur. J. Cancer.* 42:410–414.

Blom, J.W., J.P. Vanderschoot, M.J. Oostindiër, S. Osanto, F.J. van der Meer, and F.R. Rosendaal. 2006b. Incidence of venous thrombosis in a large cohort of 66,329 cancer patients: results of a record linkage study. *J. Thromb. Haemost.* 4:529–535.

Chamouard, P., D. Desprez, B. Hugel, C. Kunzelmann, C. Gidon-Jeangirard, M. Lessard, R. Baumann, J.M. Freyssinet, and L. Grunebaum. 2005. Circulating cell-derived microparticles in Crohn's disease. *Dig. Dis. Sci.* 50:574–580.

Combes, V., A.C. Simon, G.E. Grau, D. Arnoux, L. Camoin, F. Sabatier, M. Mutin, M. Sanmarco, J. Sampol, and F. Dignat-George. 1999. In vitro generation of endothelial microparticles and possible prothrombotic activity in patients with lupus anticoagulant. *J. Clin. Invest.* 104:93–102.

Corbett, T.H., B.J. Roberts, W.R. Leopold, J.C. Peckham, L.J. Wilkoff, D.P. Griswold Jr., and F.M. Schabel Jr. 1984. Induction and chemotherapeutic response of two transplantable ductal adenocarcinomas of the pancreas in C57BL/6 mice. *Cancer Res.* 44:717–726.

Davila, M., A. Amirkhosravi, E. Coll, H. Desai, L. Robles, J. Colon, C.H. Baker, and J.L. Francis. 2008. Tissue factor-bearing microparticles derived from tumor cells: impact on coagulation activation. *J. Thromb. Haemost.* 6:1517–1524.

Del Conde, I., L.D. Bharwani, D.J. Dietzen, U. Pendurthi, P. Thiagarajan, and J.A. López. 2007. Microvesicle-associated tissue factor and Trousseau's syndrome. *J. Thromb. Haemost.* 5:70–74.

Dignat-George, F. 2006. Detection of circulating endothelial cells and endothelial progenitor cells by flow cytometry. *Cytometry B Clin. Cytom.* 70:104–105.

Dubois, C., B. Steiner, and S.C. Meyer Reigner. 2004. Contribution of PAR-1, PAR-4 and GPIbalpha in intracellular signaling leading to the cleavage of the beta3 cytoplasmic domain during thrombin-induced platelet aggregation. *Thromb. Haemost.* 91:733–742.

Dubois, C., B. Atkinson, B.C. Furie, and B. Furie. 2006a. Real time in vivo imaging of platelets during thrombus formation. *In* Platelets. A.D. Michelson, editor. Elsevier/Academic Press, Worcester, MA. 611–628.

Dubois, C., L. Panicot-Dubois, G. Merrill-Skoloff, B. Furie, and B.C. Furie. 2006b. Glycoprotein VI-dependent and -independent pathways of thrombus formation in vivo. *Blood.* 107:3902–3906.

Dubois, C., L. Panicot-Dubois, J.F. Gainor, B.C. Furie, and B. Furie. 2007. Thrombin-initiated platelet activation in vivo is vWF independent during thrombus formation in a laser injury model. *J. Clin. Invest.* 117:953–960.

Dvorak, H.F., S.C. Quay, N.S. Orenstein, A.M. Dvorak, P. Hahn, A.M. Bitzer, and A.C. Carvalho. 1981. Tumor shedding and coagulation. *Science.* 212:923–924.

Falati, S., Q. Liu, P. Gross, G. Merrill-Skoloff, J. Chou, E. Vandendries, A. Celi, K. Croce, B.C. Furie, and B. Furie. 2003. Accumulation of tissue factor into developing thrombi in vivo is dependent upon microparticle P-selectin glycoprotein ligand 1 and platelet P-selectin. *J. Exp. Med.* 197:1585–1598.

Fujii, Y., M. Sekiguchi, Y. Shiroko, H. Shimizu, I. Sugawara, K. Hasumi, M. Eriguchi, T. Ikeuchi, and H. Uchida. 1990. Establishment and characterization of human pancreatic adenocarcinoma cell line SOJ producing carcinoembryonic antigen and carbohydrate antigen 19-9. *Hum. Cell.* 3:31–36.

Furie, B., and B.C. Furie. 2006. Cancer-associated thrombosis. *Blood Cells Mol. Dis.* 36:177–181.

Gasic, G.J., P.A. Koch, B. Hsu, T.B. Gasic, and S. Niewiarowski. 1976. Thrombogenic activity of mouse and human tumors: effects on platelets, coagulation, and fibrinolysis, and possible significance for metastases. *Z. Krebsforsch. Klin. Onkol. Cancer Res. Clin. Oncol.* 86:263–277.

Ghosh, A., W. Li, M. Febbraio, R.G. Espinola, K.R. McCrae, E. Cockrell, and R.L. Silverstein. 2008. Platelet CD36 mediates interactions with endothelial cell-derived microparticles and contributes to thrombosis in mice. *J. Clin. Invest.* 118:1934–1943.

Haas, S.L., R. Jesnowski, M. Steiner, F. Hummel, J. Ringel, C. Burstein, H. Nizze, S. Liebe, and J.M. Löhr. 2006. Expression of tissue factor in pancreatic adenocarcinoma is associated with activation of coagulation. *World J. Gastroenterol.* 12:4843–4849.

Hron, G., M. Kollars, H. Weber, V. Sagaster, P. Quehenberger, S. Eichinger, P.A. Kyrle, and A. Weltermann. 2007. Tissue factor-positive microparticles: cellular origin and association with coagulation activation in patients with colorectal cancer. *Thromb. Haemost.* 97:119–123.

Kakkar, A.K., and R.C. Williamson. 1999. Prevention of venous thromboembolism in cancer patients. *Semin. Thromb. Hemost.* 25:239–243.

Kaplan, R.N., S. Rafii, and D. Lyden. 2006. Preparing the "soil": the premetastatic niche. *Cancer Res.* 66:11089–11093.

Khorana, A.A., S.A. Ahrendt, C.K. Ryan, C.W. Francis, R.H. Hruban, Y.C. Hu, G. Hostetter, J. Harvey, and M.B. Taubman. 2007. Tissue factor expression, angiogenesis, and thrombosis in pancreatic cancer. *Clin. Cancer Res.* 13:2870–2875.

Kim, H.K., K.S. Song, Y.S. Park, Y.H. Kang, Y.J. Lee, K.R. Lee, H.K. Kim, K.W. Ryu, J.M. Bae, and S. Kim. 2003. Elevated levels of circulating platelet microparticles, VEGF, IL-6 and RANTES in patients with gastric cancer: possible role of a metastasis predictor. *Eur. J. Cancer.* 39:184–191.

Lacroix, R., F. Sabatier, A. Mialhe, A. Basire, R. Pannell, H. Borghi, S. Robert, E. Lamy, L. Plawinski, L. Camoin-Jau, et al. 2007. Activation of plasminogen into plasmin at the surface of endothelial microparticles: a mechanism that modulates angiogenic properties of endothelial progenitor cells in vitro. *Blood.* 110:2432–2439.

Langer, F., B. Spath, K. Haubold, K. Holstein, G. Marx, J. Wierecky, T.H. Brümmendorf, J. Dierlamm, C. Bokemeyer, and B. Eifrig. 2008. Tissue factor procoagulant activity of plasma microparticles in patients with cancer-associated disseminated intravascular coagulation. *Ann. Hematol.* 87:451–457.

Milsom, C., J. Yu, L. May, B. Meehan, N. Magnus, K. Al-Nedawi, J. Luyendyk, J. Weitz, P. Klement, G. Broze, et al. 2007. The role of tumor-and host-related tissue factor pools in oncogene-driven tumor progression. *Thromb. Res.* 120(Suppl. 2):S82–S91.

Müller, I., A. Klocke, M. Alex, M. Kotzsch, T. Luther, E. Morgenstern, S. Zieseniss, S. Zahler, K. Preissner, and B. Engelmann. 2003. Intravascular tissue factor initiates coagulation via circulating microvesicles and platelets. *FASEB J.* 17:476–478.

Myers, D.D., A.E. Hawley, D.M. Farris, S.K. Wrobleski, P. Thanaporn, R.G. Schaub, D.D. Wagner, A. Kumar, and T.W. Wakefield. 2003. P-selectin and leukocyte microparticles are associated with venous thrombogenesis. *J. Vasc. Surg.* 38:1075–1089.

Neoptolemos, J.P., D.D. Stocken, J.A. Dunn, J. Almond, H.G. Beger, P. Pederzoli, C. Bassi, C. Dervenis, L. Fernandez-Cruz, F. Lacaine, et al; European Study Group for Pancreatic Cancer. 2001. Influence of resection margins on survival for patients with pancreatic cancer treated by adjuvant chemoradiation and/or chemotherapy in the ESPAC-1 randomized controlled trial. *Ann. Surg.* 234:758–768.

Ni, H., P.S. Yuen, J.M. Papalia, J.E. Trevithick, T. Sakai, R. Fässler, R.O. Hynes, and D.D. Wagner. 2003. Plasma fibronectin promotes thrombus growth and stability in injured arterioles. *Proc. Natl. Acad. Sci. USA.* 100:2415–2419.

Panicot-Dubois, L., M. Aubert, C. Franceschi, E. Mas, F. Silvy, C. Crotte, J.P. Bernard, D. Lombardo, and M.O. Sadoulet. 2004. Monoclonal antibody 16D10 to the C-terminal domain of the feto-acinar pancreatic protein binds to membrane of human pancreatic tumoral SOJ-6 cells and inhibits the growth of tumor xenografts. *Neoplasia.* 6:713–724.

Panicot-Dubois, L., G.M. Thomas, B.C. Furie, B. Furie, D. Lombardo, and C. Dubois. 2007. Bile salt-dependent lipase interacts with platelet CXCR4 and modulates thrombus formation in mice and humans. *J. Clin. Invest.* 117:3708–3719.

Pawlinski, R., and N. Mackman. 2008. Use of mouse models to study the role of tissue factor in tumor biology. *Semin. Thromb. Hemost.* 34:182–186.

Piccin, A., W.G. Murphy, and O.P. Smith. 2007. Circulating microparticles: pathophysiology and clinical implications. *Blood Rev.* 21:157–171.

Prandoni, P., A.W. Lensing, H.R. Büller, A. Cogo, M.H. Prins, A.M. Cattelan, S. Cuppini, F. Noventa, and J.W. ten Cate. 1992. Deep-vein thrombosis and the incidence of subsequent symptomatic cancer. *N. Engl. J. Med.* 327:1128–1133.

Riewald, M., and W. Ruf. 2001. Mechanistic coupling of protease signaling and initiation of coagulation by tissue factor. *Proc. Natl. Acad. Sci. USA.* 98:7742–7747.

Robert, S., P. Poncelet, R. Lacroix, L. Arnaud, L. Giraudo, A. Hauchard, J. Sampol, and F. Dignat-George. 2009. Standardization of platelet-derived microparticle counting using calibrated beads and a Cytomics FC500 routine flow cytometer: a first step towards multicenter studies? *J. Thromb. Haemost.* 7:190–197.

Sabatier, F., P. Darmon, B. Hugel, V. Combes, M. Sanmarco, J.G. Velut, D. Arnoux, P. Charpiot, J.M. Freyssinet, C. Oliver, et al. 2002. Type 1 and type 2 diabetic patients display different patterns of cellular microparticles. *Diabetes.* 51:2840–2845.

Sack, G.H., Jr., J. Levin, and W.R. Bell. 1977. Trousseau's syndrome and other manifestations of chronic disseminated coagulopathy in patients with neoplasms: clinical, pathophysiologic, and therapeutic features. *Medicine (Baltimore).* 56:1–37.

Schiavetti, A., M. Foco, A. Ingrosso, E. Bonci, L. Conti, and M. Matrunola. 2008. Venous thrombosis in children with solid tumors. *J. Pediatr. Hematol. Oncol.* 30:148–152.

Sierko, E., and M.Z. Wojtukiewicz. 2007. Inhibition of platelet function: does it offer a chance of better cancer progression control? *Semin. Thromb. Hemost.* 33:712–721.

Stein, P.D., A. Beemath, F.A. Meyers, E. Skaf, J. Sanchez, and R.E. Olson. 2006. Incidence of venous thromboembolism in patients hospitalized with cancer. *Am. J. Med.* 119:60–68.

Tesselaar, M.E., F.P. Romijn, I.K. Van Der Linden, F.A. Prins, R.M. Bertina, and S. Osanto. 2007. Microparticle-associated tissue factor activity: a link between cancer and thrombosis? *J. Thromb. Haemost.* 5:520–527.

Tilley, R.E., T. Holscher, R. Belani, J. Nieva, and N. Mackman. 2008. Tissue factor activity is increased in a combined platelet and microparticle sample from cancer patients. *Thromb. Res.* 122:604–609.

Trousseau, A. 1865. Phlegmasia alba dolens. *In* Clinique Médicale de l'Hôtel-Dieu. J.-B. Baillière, Paris. 654–712.

Vandendries, E.R., J.R. Hamilton, S.R. Coughlin, B. Furie, and B.C. Furie. 2007. Par4 is required for platelet thrombus propagation but not fibrin generation in a mouse model of thrombosis. *Proc. Natl. Acad. Sci. USA.* 104:288–292.

Versteeg, H.H., F. Schaffner, M. Kerver, H.H. Petersen, J. Ahamed, B. Felding-Habermann, Y. Takada, B.M. Mueller, and W. Ruf. 2008. Inhibition of tissue factor signaling suppresses tumor growth. *Blood.* 111:190–199.

Willekens, F.L., J.M. Werre, J.K. Kruijt, B. Roerdinkholder-Stoelwinder, Y.A. Groenen-Döpp, A.G. van den Bos, G.J. Bosman, and T.J. van Berkel. 2005. Liver Kupffer cells rapidly remove red blood cell-derived vesicles from the circulation by scavenger receptors. *Blood.* 105:2141–2145.

Yu, J.L., L. May, V. Lhotak, S. Shahrzad, S. Shirasawa, J.I. Weitz, B.L. Coomber, N. Mackman, and J.W. Rak. 2005. Oncogenic events regulate tissue factor expression in colorectal cancer cells: implications for tumor progression and angiogenesis. *Blood.* 105:1734–1741.

Zwicker, J.I., B.C. Furie, and B. Furie. 2007. Cancer-associated thrombosis. *Crit. Rev. Oncol. Hematol.* 62:126–136.